

AD-766 251

GROWTH AND HARDENING OF ALKALI HALIDES FOR
USE IN INFRARED LASER WINDOWS

William A. Sibley, et al

Oklahoma State University

Prepared for:

Air Force Cambridge Research Laboratories

30 April 1973

DISTRIBUTED BY:

NTIS

National Technical Information Service
U. S. DEPARTMENT OF COMMERCE
5285 Port Royal Road, Springfield Va. 22151

GROWTH AND HARDENING OF ALKALI HALIDES FOR
USE IN INFRARED LASER WINDOWS

by

William A. Sibley, Charles T. Butler, John R. Hopkins

Joel J. Martin, Joe A. Miller

Department of Physics
Oklahoma State University
Stillwater, Oklahoma 74074

Contract No. F19628-72-C-0306

Annual Technical Report

30 April 1973

Contract Monitor: Normantas Klausutis, Captain, USAF
Solid State Sciences Laboratory

Approved for public release; distribution unlimited.

Sponsored by
Defense Advanced Research Projects Agency
ARPA Order No. 2055

Monitored by
AIR FORCE CAMBRIDGE RESEARCH LABORATORIES
AIR FORCE SYSTEMS COMMAND
UNITED STATES AIR FORCE
BEDFORD, MASSACHUSETTS 01730

AD 766251

R

ARPA Order No. 2055

Program Code No. 2D10

Contractor:
Oklahoma State University

Effective Date of Contract:
1 May 1972

Contract No. F19628-72-C-0306

Principal Investigator & Phone No.:
Dr. W. A. Sibley
(405) 372-6211, x7525

AFCRL Project Scientist & Phone No.:
Capt. Norwantas Klausutis
(617) 861-4841

Contract Expiration Date:
30 April 1975

A

Qualified requestors may obtain additional copies from
the Defense Documentation Center. All others should
apply to the National Technical Information Service.

Unclassified

Security Classification

DOCUMENT CONTROL DATA - R & D		
(Security classification of title, body of abstract and indexing annotation must be entered when the overall report is classified)		
1. ORIGINATING ACTIVITY (Corporate author) Oklahoma State University Department of Physics Stillwater, Oklahoma 74074		2a. REPORT SECURITY CLASSIFICATION Unclassified 2b. GROUP N/A
3. REPORT TITLE GROWTH AND HARDENING OF ALKALI HALIDES FOR USE IN INFRARED LASER WINDOWS		
4. DESCRIPTIVE NOTES (Type of report and inclusive dates) Scientific Interim.		
5. AUTHOR(S) (First name, middle initial, last name) William A. Sibley Joel J. Martin Charles T. Butler Joe A. Miller John R. Hopkins		
6. REPORT DATE 30 April 1973	7a. TOTAL NO. OF PAGES 49	7b. NO. OF REFS 24
8a. CONTRACT OR GRANT NO. F19628-72-C-0306 8. PROJECT NO. Project, Task, Work Unit Nos. c. 2055 n/a n/a DoD Element 61101D d. DoD Subelement n/a		9a. ORIGINATOR'S REPORT NUMBER(S) Annual Technical Report 9b. OTHER REPORT NO(S) (Any other numbers that may be assigned this report) AFCRL-TR-73-0342
10. DISTRIBUTION STATEMENT A - Approved for public release; distribution unlimited.		
11. SUPPLEMENTARY NOTES This research was supported by the Defense Advanced Research Projects Agency.		12. SPONSORING MILITARY ACTIVITY Air Force Cambridge Research Laboratories (LQ) L. G. Hanscom Field Bedford, Massachusetts 01730
13. ABSTRACT Several undoped and Sr doped KCl crystals have been grown from reagent grade powder in a crystal puller recently placed in operation. The Sr concentration in the doped crystals was varied from a few up to 650 parts per million (ppm) molar. The engineering flow stresses or yield points of these reagent grade crystals have been measured. Values obtained range from 300 psi for undoped crystals to 2550 psi for the most heavily doped crystal. These results, as well as the Vickers micro-hardness results, are in good agreement with measurements on crystals grown at Oak Ridge National Laboratory (ORNL) using purified powders. The flow stress of high purity KCl from ORNL is found to increase from an unirradiated value of 300 psi to 2700 psi at an electron radiation dose which has introduced a Cl^0 interstitial concentration of 65 ppm. The increase in flow stress is directly proportional to the square root of the defect concentration for both Sr doped and irradiated KCl crystals. This result is in good agreement with Fleischer's theory.		

DD FORM 1473
1 NOV 65

Unclassified

Security Classification

ia

Unclassified
Security Classification

14 KEY WORDS	LINK A		LINK B		LINK C	
	NO. 1	WT	NO. 1	WT	NO. 1	WT
Alkali Halides Pure and doped KCl KCl:KBr mixed crystals Flow Stress Vickers Hardness Wing Size Crystal Growth Crystal Characterization Irradiated KCl						

Unclassified
Security Classification

GROWTH AND HARDENING OF ALKALI HALIDES FOR
USE IN INFRARED LASER WINDOWS

by

William A. Sibley, Charles T. Butler, John R. Hopkins

Joel J. Martin, Joe A. Miller

Department of Physics
Oklahoma State University
Stillwater, Oklahoma 74074

Contract No. F19628-72-C-0306

Annual Technical Report

30 April 1973

Contract Monitor: Normantas Klausutis, Captain, USAF
Solid State Sciences Laboratory

Approved for public release; distribution unlimited.

Sponsored by
Defense Advanced Research Projects Agency
ARPA Order No. 2055
Monitored by
AIR FORCE CAMBRIDGE RESEARCH LABORATORIES
AIR FORCE SYSTEMS COMMAND
UNITED STATES AIR FORCE
BEDFORD, MASSACHUSETTS 01730

ABSTRACT

Several undoped and Sr doped KCl crystals have been grown from reagent grade powder in a crystal puller recently placed in operation. The Sr concentration in the doped crystals was varied from a few up to 650 parts per million (ppm) molar. The engineering flow stresses or yield points of these reagent grade crystals have been measured. Values obtained range from 300 psi for undoped crystals to 2550 psi for the most heavily doped crystal. These results, as well as the Vickers microhardness results, are in good agreement with measurements on crystals grown at Oak Ridge National Laboratory (ORNL) using purified powders. The flow stress of high purity KCl from ORNL is found to increase from an unirradiated value of 300 psi to 2700 psi at an electron radiation dose which has introduced a Cl^0 interstitial concentration of 65 ppm. The increase in flow stress is directly proportional to the square root of the defect concentration for both Sr doped and irradiated KCl crystals. This result is in good agreement with Fleischer's theory.

I. INTRODUCTION

This project was initiated to study the effects of doping and electron irradiation on the mechanical and optical properties of alkali halides. Our group has concentrated its efforts on KCl, which has been shown to be the most promising material for use in CO₂ laser windows. A significant part of the Oklahoma State University project involves growth of crystals. This area may be separated into two broad aims: comparison of various properties among single crystals grown from identical starting material in one of two different types of apparatus, and comparison of these properties among crystals grown in a particular apparatus using starting material prepared in several different manners.

The second major area of the project consists of determining changes in mechanical and optical properties of KCl doped with selected impurities, irradiated with 1.5 MeV electrons or treated in one of several other ways. Mechanical properties monitored include the flow stress, measured both in compression and in bending, the Vickers microhardness, and the dislocation rosette size obtained upon indentation of the crystal by the Vickers stylus. The principal optical property determined is the absorption coefficient at 10.6 μ m. These measurements are carried out in cooperation with AFCRL and other laboratories.

II. CRYSTAL GROWTH

A. Introduction

One of the two primary activities of the crystal growth phase of this project is simply to provide pure and doped crystals from which

samples may be taken to perform mechanical and optical tests. All crystals grown for the project at this institution so far have utilized untreated, reagent grade KCl powder.* Crystals will presently be grown in the same type of apparatus utilizing both high purity starting material treated with HCl and Cl₂ gases and reagent grade material treated to remove hydroxyl ions and other oxygen compounds. If, for instance, it can be demonstrated that no significant advantage is gained by using the high purity starting material over treated, reagent grade powder, a significant economy will have been effected. Trace cation and anion impurities may prove to contribute significantly to the 10.6 μ m absorption. This can be demonstrated most conclusively if the crystals are grown in the same or in essentially identical apparatus.

A second important aim of the crystal growth portion of the project is comparison of crystals grown from identical starting material using both pulling and Bridgman apparatus. A pulling technique is normally used to obtain research specimens, while large ingots to be used either for rolling, pressing or directly as laser windows would most likely be grown by the Bridgman method. For several reasons, crystals grown by the two methods might be expected to have differing properties. Impurity segregation patterns and void concentrations, for instance, are known to be quite different in KCl grown by the two methods.

B. Apparatus

Three separate apparatus are necessary to meet the aims of the

*Crystals grown from this type of starting material will be referred to as "reagent grade" to distinguish them from crystals grown using specially purified starting material, or from reagent grade powder treated to remove oxygen compounds.

project. The first crystal puller has been in operation for several months; the second puller undergoing installation. The third apparatus, of the Bridgman type, is nearing completion in the Physics-Chemistry Machine Shop.

Model I Puller. General features of the Model I Puller are shown in Figure 1. The graphite heater consists of a slotted cylindrical portion and a slotted flat pedestal section, electrically connected in series. In operation, these heaters typically dissipate 250 W at a current of 45 A. The cylindrical heater is maintained at a preset temperature by an external three action controller (Research, Incorporated, Model 625). The sensing element is a type K thermocouple embedded in the cylinder wall. A second thermocouple is used to monitor the pedestal (base) heater temperature. In order to maintain the proper temperature profile in the melt, the base heater is operated 50 to 100°C above that of the cylinder heater. Both heaters are mounted on nickel blocks which are mechanically clamped to the water-cooled base plate by the current feed throughs. BeO washers provide the necessary low electrical and high thermal conductance.

The entire heater assembly is enclosed in a double-walled, water-cooled, stainless steel vacuum jacket. To facilitate observation of the growth interface, a microscope illumination lamp is permanently mounted to one of the three view ports on the top plate. High purity alumina crucibles (Coors Porcelain, grade AD99) 5cm diameter by 9cm high are presently employed. A water-cooled, stainless steel pullrod with an integral nickel seed chuck is used. A separate seed chuck cannot be used in this system since the heat of solidification is removed through the seed and crystal during a significant portion of the growth process.

The pullrod is rotated at 30 rpm by a small motor located on the lift mechanism. In this way, small radial assymetries in the temperature distribution within the heater volume are smoothed out, and a more symmetric crystal is obtained. The heater and current feedthrough designs are similar to ones in use by F. Rosenberger (1) at the University of Utah. The pullrod, vacuum seals, lift mechanism and other features were developed here.

Pulling is accomplished by moving the pullrod and its rotation motor with a precision lead screw driven by a variable speed motor. Precision linear ball bearings insure smooth motion. The lift rate is directly readable from a calibrated tachometer, and is continuously adjustable from zero up to 1.8cm/hr. An electromechanical clutch allows manual adjustment of the pullrod position when necessary.

Model II Puller. Figure 2 shows the second pulling apparatus. In this design, no thermocouples, heaters or other hardware are mounted within the vacuum enclosure. This results in less contamination of high purity melts and facilitates clean-up after a doped crystal is grown. The only materials which are at full temperature are the crucible, its silica stand, and the high purity silica vacuum enclosure. A type K thermocouple, placed at a suitable level on the outside wall of the silica enclosure, serves as the sensing element for the temperature controller. The same controller is used interchangeably for both pullers. The pullrod and vacuum connections are made to the silica envelope by means of a water-cooled, stainless steel header. The basic design for this system is similar to one developed by one of the authors (CTB) at Oak Ridge National Laboratory for high purity KCl single crystals (2, 3). The mechanical pulling mechanism and pullrod are essentially identical

to those for the first puller.

The vacuum systems for both pullers are separate but identical, sharing only a common fore pump. Each system comprises a 2-inch, water-cooled and baffled diffusion pump (T-M Vacuum Products) and a liquid nitrogen cold trap (Circuits Processing Apparatus). The T-M diffusion pump has a three minute start up and a one minute cool down time.

Because operation of these apparatus requires several pump-down and inert gas backfills, this feature results in a considerable time saving.

In a typical growth run using reagent material, approximately 110 g KCl powder is transferred directly from a supply bottle into a crucible. For Sr-doped crystals, the appropriate amount of anhydrous SrCl_2 is added. The crucible is then placed in the heater assembly on 20mm ceramic standoffs and carefully centered. A seed 5x5x30mm is secured in the chuck, the apparatus assembled, and the enclosure evacuated to a pressure near 10^{-5} torr. The system is then backfilled once with argon gas, repumped, and baked under hard vacuum overnight at 300°C .

The next morning, the system is flushed with argon gas, repumped to hard vacuum, and the temperature raised to 700°C . Often, one or more additional argon backfills are employed during the hour required to reach this temperature. At 700°C , the system is sealed at a static argon pressure of 20-25 torr absolute. This pressure is sufficient to suppress evaporation from the melt, but insufficient to allow significant convective transport. Thus, the viewports remain clear throughout the growth run. Pulling rates up to 1cm/hr are possible during the early stages of growth in this apparatus, but as the crystal lengthens, pull rates must be lowered because of the lessened heat conductance. Later, as radiative losses from the interface and crystal body become

important, pull rates of 1.5cm/hr or greater may be used. A significant difference in the designs of the two pulling apparatus lies in the manner in which the heat of solidification is removed from the growth interface. In the number two puller, radiative losses predominate during the entire growth process, and relatively high pull rates are continuously maintainable.

In previous work, it has been found necessary to use apparatus capable of being evacuated to 10^{-5} torr or below if oxygen compounds are to be excluded from pure crystals, and if unwanted precipitation of dopants is to be avoided in doped runs. That is, if air is allowed to contact the melt during growth, or if the starting material is insufficiently outgassed, pure crystals tend to be oxygen and hydroxyl doped, while doped crystals tend to be purer than desired.

Bridgman System. The third crystal growth apparatus, now being constructed in the Physics-Chemistry Machine Shop, is of a modified Bridgman design. Mechanical motion, although much slower in this equipment, will be accomplished by a lead screw and motor system essentially identical to that used on the pullers. The crucible will be lowered through the stationary furnace on a water-cooled, nickel pedestal. Again, the system will be vacuum tight, and will run under a small argon pressure.

C. Characterization

Figure 3 is a photograph of three typical reagent grade crystals grown in puller 1. They are of (100) orientation and nearly square in cross section. Crystals as large as 3cm on a side with masses to 100g have been grown in this apparatus; larger ones can be grown with puller

number 2.

Etch-pit counts on slabs cleaved from these crystals reveal dislocation densities typical for Czochralski grown KCl crystals--
 $2-5 \times 10^5 \text{ cm}^{-2}$. No general chemical analyses have been made on the untreated reagent crystals; but optical spectroscopy indicates that both the undoped and the Sr doped crystals contain typically $1 \mu\text{g/g}$ hydroxyl. The hydroxyl content was estimated from the 204nm absorption band in KCl using the relation

$$C_{\text{OH}} = 1.31 A/t \quad (1)$$

where A is the optical density at the peak of the 204nm band; t is the sample thickness in cm and C_{OH} is the concentration in $\mu\text{g OH}^-$ per g KCl (4). For the concentration to be expressed in molar ppm, the numerical coefficient should be changed to 5.75.

Table I presents a list of crystals grown to date on this project, together with their disposition and dopant concentration, if applicable. The Sr analyses were performed in the Oklahoma State University Soil Test Laboratory by atomic absorption spectroscopy. The Sr concentrations given in the table are those in the upper and lower portions of the boule, respectively. Because of impurity banding and other effects, the reported concentrations are probably not good to better than 25-50%, even though the individual analyses are much more reliable than this.

Figure 4 presents a plot of the measured molar concentrations of Sr at the top, middle, and bottom of each of several crystals versus the initial Sr concentration in the melts. The effective segregation coefficient for Sr in KCl, using this apparatus, is seen to lie between about 0.1 and 0.2. This is in agreement with values found earlier by Kelting and Witt (5) and by Sibley and Russell (6).

TABLE I
CRYSTALS

Crystal No.	Dopant ($\mu\text{g/g}$)	Disposition
022273	undoped	mechanical tests
022373	"	mechanical tests & AFCRL optical tests
022873	"	NRL optical tests
030973	"	mechanical tests
031473	66 to 160, Sr	mechanical tests
032873	270 to 500, Sr	mechanical tests, AFCRL & NRL optical tests
040473	540 to 770, Sr	mechanical tests & AFCRL optical tests
041173 ^a	—Sr	---
041373 ^a	—Sr	---
041873 ^a	—Sr	---

^a Not yet analyzed

III. MECHANICAL PROPERTIES

A. Introduction

It is well known that tetragonal defects such as those introduced by ionizing radiation or divalent impurity vacancy pairs cause a significant strengthening of alkali halide single crystals (7, 8, 9). Fleischer (10) has shown theoretically that the increase in flow stress due to the strain field of tetragonal defect is proportional to the square root of the defect concentration. While the details of the theory are complex, the concentration dependence can be easily found. The crystal yields under stress by dislocations moving along their slip plane; thus, we

must consider the interaction between the dislocations and the defects. If the interaction is short ranged, and if the defect concentration is small, we need only consider those defects which lie on the slip plane. Therefore, if each defect can exert some maximum force, F_m , on a dislocation, then the maximum force per unit length of dislocation is F_m/l , where l is the average distance between defects. In order to move the dislocation, the applied stress must increase an amount F_m/bl , where b is the Burger's vector. If A is the area occupied by the defect on the slip plane, the atomic concentration, C , is A/l^2 ; and the resulting stress increase, $\Delta\tau$, is given by

$$\Delta\tau = \frac{F_m C^{\frac{1}{2}}}{bA^{\frac{1}{2}}} \quad (2)$$

Fleischer related F_m to the shear modulus, G , and to geometrical factors. In simplified form, the increase in the flow stress predicted by his theory can be written as

$$\Delta\tau = (G/n)C^{\frac{1}{2}} \quad (3)$$

with $n = 10$ and 100 for interstitials and divacancies respectively.

Equation 3 can be expected to break down when the defect concentration becomes large as in the case of mixed crystals such as the KCl_xBr_{1-x} materials. Later in this report a comparison will be made between Fleischer's theory and the hardening results of Sr doped and irradiated KCl crystals.

Since a small grain size inhibits plastic flow, single crystals can be hardened by methods which convert it to fine grain material. Techniques such as press forging or pressure-induced recrystallization are used. The flow stress, τ , of polycrystalline material is given by the Petch (11) relation

$$\tau = \tau_0 + kd^{-\frac{1}{2}} \quad (4)$$

where τ_0 is the flow stress of the single crystal, k is a constant and d is the average grain size. Rice (12) has shown that press forging effectively hardens KCl and has pointed out that Sr doping should provide an additional increase in τ , since it will increase τ_0 . Hence, our Sr doping and irradiation results should provide valuable data for the forging work.

B. Measurement Methods

The mechanical strength of the samples was measured with four different test techniques. They are the uniaxial compression test, the four point bend test, the Vickers microhardness test and the dislocation rosette size test. Of these tests, only the Vickers microhardness test does not give the flow stress (yield point).

Compression Tests. The uniaxial compression tests were run on an Instron testing machine which recorded the applied force as the sample was being compressed at a constant strain rate. Flow-stress samples were cleaved from single crystal ingots; each sample measured approximately 1.5mm x 2mm x 7mm. Since the sample length was at least three times the width, possible end effects were small. Samples were compressed along a $\langle 100 \rangle$ direction at a crosshead speed of 0.05 cm/min. This corresponds to a strain rate of approximately 10^{-3} sec^{-1} . Figure 5 shows a typical stress-strain curve for purified KCl boule P-1. As shown, the engineering flow stress, τ_e , is taken to be the stress value at the intersection of tangents to the elastic and first plastic portions of the curve. The individual flow stresses of at least five samples were averaged to obtain the values reported for each material.

In order to compare the results with theory, the resolved flow stress, τ_r , that is, the component of the flow stress parallel to the primary slip direction, is needed. Since the primary slip direction is $\langle 110 \rangle$ in KCl, $\tau_r = \frac{1}{2}\tau_e$.

Four Point Bend Tests. The flow stress can also be measured under tension and by bending. Since it is difficult to attach grips to small KCl crystals for tension measurements, we have made some four point bend tests to complement our compression tests. Figure 6 shows the four point bend jig which was mounted on the Instron's load cell. The sample undergoes pure bending between the inner loading points which gives a non-uniform stress on the sample. The stress varies from tension (top) to compression (bottom) across the sample. In the elastic region, the maximum stress, τ_m , (on either the upper or lower edge) is given by

$$\tau_m = 3Pd/wt^2 \quad (5)$$

where P is the load, w is the width of the sample, and d and t are the dimensions shown. Equation 5 can then be used to find the flow stress as measured under compression. The single crystal samples were freshly cleaved along $\langle 100 \rangle$ directions. Each sample measured approximately 2mm x 5mm x 10mm. For the bend tests, the crosshead speed was lowered to 0.005cm/min. Figure 7 shows a typical stress-strain curve for the bend tests. Figure 8 compares the resolved flow stress as measured by four point bend and uniaxial compression tests. Since the tests agree to within the experimental uncertainty of the measurements, and since the bend tests require considerably more sample material, we will utilize only compression tests in the future.

Microhardness and Rosette Size Tests. Microhardness tests and flow stress measurements are techniques commonly used to determine the

mechanical strength of a material. Davisson and Vaughan (13) have shown that the size of the dislocation rosette produced around a microhardness indentation is a useful and convenient test for determining mechanical strengths of single crystals since the size of the rosette should be inversely proportional to the flow stress and since this test can be performed at essentially the same time as the microhardness measurements. Groves and Fine (14) and Davidge (15) have used the rosette size to measure the strength of Fe doped MgO. Davidge found that for heavily doped material the rosette size was indeed inversely proportional to the flow stress in KCl. Although hardening mechanisms have been studied using the rosette size (16) few intercomparisons between flow stress, microhardness, and rosette size have been made on the same samples. KCl is an excellent material for an investigation of techniques for measuring mechanical strengths, since large pure or doped single crystals are readily available and since considerable work on the mechanical properties of pure and doped KCl has already been done (7, 8, 9). The purpose of this experiment was to compare flow stress, Vickers microhardness, and dislocation rosette size measurements for purified KCl single crystals, KCl:Ca, KCl:Sr, and $\text{KCl}_{1-x}\text{Br}_x$ mixed single crystals.

A Leitz Miniload tester with a Vickers type diamond indenter was used for the microhardness and rosette (wing) size tests. In order to facilitate dislocation etching the indentations were made on freshly cleaved {100} faces in a glove box in which the absolute humidity was held under 8g/m^3 . The diagonals of the indentations were along the $\langle 100 \rangle$ directions. The hardness numbers (Table II) were obtained from an average of at least five indentations for loads of 5g, 10g, 15g, and 25g; these hardness numbers were found to be essentially independent of

TABLE II
RESOLVED FLOW STRESS, τ_r ; VICKERS HARDNESS, HV; AND WING SIZE, W_o

Material	Dopant (ppm)	τ_r (kg/mm ²)	HV (kg/mm ²)	W_o (μ m)
KCl-P-1	Purified	0.11	9.2	91
KCl-P-2	Purified	0.15	9.0	91
KCl-Ca-1	100 Ca	0.20	11.2	77
KCl-Ca-2	540 Ca	0.55	16.7	41
KCl-Sr-1	50-150 Sr	0.23	13.0	77
KCl-Sr-2	470 Sr	0.57	16.9	41
KCl-Sr-3	138 Sr	0.38	14.9	60
KCl 33% - KBr 67%		0.89	21.2	24
KCl 75% - KBr 25%		0.96	19.8	24

load for loads of 5g to 50g.

The dislocation rosettes (Fig. 9) around the indentations were revealed by etching the sample momentarily (1 s to 3 s), rinsing it in acetone, and then blotting it dry. Glacial acetic acid was found to be the best etchant for the pure materials while a saturated solution of BaBr₂ in absolute methanol was more effective for the doped samples. The glacial acetic acid would also etch the doped crystals but it was considerably slower. The rosette size, or wing length, W, was taken as the length from the center of the indentation to the wing tip along a $\langle 110 \rangle$ direction.

The relationship between the Vickers hardness number, HV, and the resolved flow stress, τ_r , measured on the same sample of each of the different crystals including a pure KBr crystal is portrayed in Figure

10. It is not surprising that HV is not directly proportional to τ_r since the indenter activates both the primary $\langle 110 \rangle$ and secondary $\langle 100 \rangle$ slip systems while the resolved flow stress measures only the stress necessary to move dislocations along the primary slip system. The hardness numbers and flow stress values for the purified and doped KCl are in substantial agreement with those reported by Chin et al. (17).

Figure 11 indicates that the dislocation rosette size, W , is directly proportional to the load on the indenter. Inspection of the figure suggests that there should be a finite wing size, W_0 , for zero indenter load. This result can be qualitatively understood when the nature of the microhardness test is considered. In this test, a dead-weight loaded pyramidal diamond indenter is allowed to slowly contact the surface of the crystal. The indenting diamond generates a string of fresh dislocations. The first of these dislocations is forced out by succeeding ones to a distance for which the applied stress on the string just equals the minimum stress needed to move dislocations along the primary slip direction, τ_r . Thus, the greater τ_r , the smaller W . The maximum stress on the crystal occurs at the instant the indenter contacts the sample and the dislocations immediately move out a distance W_0 , since the dislocation velocity is very much greater than the indenter velocity (7). This conjecture is further substantiated by the results of E. Aerts et al. (18) who, while studying the mobility of dislocations in X-irradiated NaCl, established that the wing size is independent of the orientation of the indentation figure. Any additional wing extent, $W - W_0$, comes about only because the indenter displaces crystal material as it moves on into the crystal. The indenter stops penetrating the crystal when the indenter stress is balanced by the rupture stress of

the crystal; hence, the initial rosette size, W_0 , is the one to be compared to the resolved flow stress. Figure 12 is a plot of the resolved flow stress, τ_r , versus $100/W_0$. It clearly shows τ_r to be inversely proportional to W_0 for larger τ_r values. The data seem to indicate that the wing sizes approach some maximum value for the softer crystals. Since the wing lengths for the softer crystals are greater than $100\mu\text{m}$, subgrain boundaries or other macroscopic crystal defects could easily be limiting the extent of the wings. Davidge's results on MgO:Fe also indicated that the flow stress is inversely proportional to the wing size except at low flow stresses where the wing size is smaller than would be expected.

For a given indenter load, τ_r is inversely proportional to W for the harder crystals, but the linear region of τ_r versus W^{-1} does not intercept the origin. This fact, combined with the fact that deviations occur for large W (soft crystals) indicates that care should be exercised when using only the dislocation rosette size technique to investigate hardening mechanisms.

For certain applications it would be useful to have a nondestructive test for the mechanical strength of a material. We have shown that there is a good correlation between the flow stress and the inverse of the length of the dislocation rosette size. Thus, once a rosette size versus flow stress calibration has been made for a particular crystal system, the rosette size becomes a useful, simple, nearly nondestructive technique for determining the flow stress of a crystal.

C. Mechanical Properties of Doped KCl

The addition of Sr to KCl causes a tetragonal defect; therefore, Sr

will strengthen the lattice. The Sr^{2+} ion preferentially occupies a K^+ lattice site. In order for the crystal to remain electrically neutral, a vacant K^+ site is also formed, which creates a Sr-vacancy pair. The vacancy is formed near the Sr^{2+} ion, since that most nearly preserves local charge neutrality.

We have measured the Vickers microhardness and the flow stress (under compression) of OSU-grown reagent grade undoped and Sr doped KCl single crystals. The characterization of the crystals is given in Section II of this report. In order to insure uniform Sr concentrations, the samples for mechanical tests were cleaved from horizontal sections of the doped crystals. Table III gives the engineering flow stress, the resolved flow stress and the Vickers microhardness not only for these crystals, but also for earlier measurements on Oak Ridge material, and on two KCl-KBr mixed crystals from AFCRL (19). The agreement between the new reagent grade crystals and the older purified Oak Ridge crystals is satisfactory--especially in view of the uncertainties in Sr concentration determinations. Also, it is interesting to note that crystals containing 650 ppm Sr have nearly the same flow stress as KCl-KBr mixed crystals. Figure 13 shows the resolved flow stress versus atomic concentration for our crystals. Engineering flow stresses are shown on the right-hand axis of the figure. The solid curve is the $C^{\frac{1}{2}}$ dependence as predicted by Fleischer's theory. It is interesting to note that the hardness, flow stress and dislocation rosette size for both the KCl-KBr crystals and the doped crystals fall on the same curves (Figs. 10 and 12), even though the hardening mechanisms must be different between these crystals.

Because the possibility of OH^- and O_2^- contamination of KCl window

TABLE III
ENGINEERING FLOW STRESS, τ_e ; RESOLVED FLOW STRESS, τ_r ; AND VICKERS
HARDNESS, HV, FOR PURE AND DOPED KCl CRYSTALS

Material	Dopant (molar ppm)	τ_e (psi)	τ_r (kg/cm ²)	HV (kg/mm ²)
022373	0	330	0.12	10.3
030973	0	240	0.086	10.0
031473B	66 Sr	750	0.27	13.2
031473D	160 Sr	1060	0.38	13.8
032873E	230 Sr	1450	0.51	15.9
032873G	370 Sr	1880	0.66	17.0
040473H	460 Sr	2160	0.76	18.2
040473J	650 Sr	2550	0.90	19.7
KCl-P-1 ^a	O-purified	320	0.11	9.2
KCl-P-2 ^a	O-purified	440	0.15	9.0
KCl-Ca-1 ^a	100 Ca	580	0.20	11.2
KCl-Ca-2 ^a	540 Ca	1600	0.55	15.6
KCl-Sr-1 ^a	50-150 Sr	660	0.23	13.0
KCl-Sr-2 ^a	470 Sr	1660	0.57	16.9
KCl-Sr-3 ^a	138 Sr	1080	0.38	14.9
KCl 33% - KBr 67% ^b		2600	0.89	21.2
KCl 75% - KBr 25% ^b		2800	0.98	19.8
KCl:OH	50 OH ⁻	454	0.16	10.8
KCl:O ₂ ^{-d}		340	0.12	11.7

^a ORNL crystal

^b AFCRL Crystal Numbers LQ218 and LQ219 respectively

^c Crystal from M. V. Klein, Physics Department, University of Illinois

^d Crystal from J. Rolfe, NRC, Ottawa

materials has been of some concern, the effects of these two impurities on mechanical properties have been investigated.* The 204nm absorption band of the hydroxyl-doped crystal indicated that the concentration of OH^- was approximately $50\mu\text{g/g}$. The only other absorption found in this sample was the infrared water absorption at $2.75\mu\text{m}$. The mechanical test data are essentially identical to those of undoped KCl and are presented in Table III. At least at the concentration available, hydroxyl contamination does not present a serious mechanical problem in undoped KCl. This result is not unexpected. Hydroxyl enters the KCl lattice substitutionally for a Cl^- ion, and at room temperature, forms a symmetric defect which has little hardening effect. Oxygen compounds, however, may very well cause undesirable optical absorption near $10.6\mu\text{m}$. The O_2^- concentration of the oxygen doped specimen has not yet been determined, but the crystal shows the 250nm absorption normally attributed to O_2^- (20), as well as hydroxyl bands at 204nm and $2.75\mu\text{m}$. The hydroxyl concentration of this oxygen-doped crystal, as determined from its ultraviolet OH^- band, is perhaps $140\mu\text{g/g}$. Again, the mechanical properties of the oxygen-doped crystal, presented in Table III, show no significant change from undoped specimens. For comparison purposes, it should be noted that the hydroxyl content of the reagent grade and purified crystals tested was typically 1 and $10^{-3}\mu\text{g/g}$, respectively.

* The hydroxyl-doped crystal, grown by F. Rosenberger, University of Utah, was obtained from Miles Klein, University of Illinois. John Rolfe of the National Research Council (Canada), supplied the O_2^- -doped crystal.

D. Radiation Hardening of Pure KCl

Another major emphasis of this project is investigation of radiation hardening of alkali halide window materials. We report here flow stress and Vickers hardness measurements as a function of radiation dose on purified KCl. Sibley and Sonder (8, 21) have shown that radiation damage occurs through a very efficient photochemical process in these materials. The damage process operates as follows: ionizing radiation removes the extra electron from a Cl^- ion which then forms an excited Cl_2^- molecule with a neighboring Cl^- ion. The molecule, upon losing its energy of excitation, breaks apart and the ions recoil along a $\langle 110 \rangle$ direction. This initiates a focusing collision sequence, the final result of which is a Cl vacancy and a Cl^0 interstitial some distance away. The Cl vacancy quickly traps an electron and becomes the so-called F center, which exhibits an absorption centered near 560nm in KCl. This absorption band can be used to determine the F center concentration, and therefore, the Cl^0 interstitial concentration, since there is a one to one correspondence between the F-center and the interstitial concentrations. The F center concentration, N_F (cm^{-3}), can be found from Smakula's relation (6, 22) (given here for a Gaussian shaped peak),

$$N_F f = 0.87 \times 10^{17} \frac{n_o}{(n_o^2 + 2)^2} \alpha_{\max} W_{\frac{1}{2}} \quad (6)$$

where f is the oscillator strength, n_o is the index of refraction, α_{\max} is the absorption coefficient at the peak of the F band, and $W_{\frac{1}{2}}(V)$ is the width at half maximum of the F absorption. (To convert F center concentrations in cm^{-3} to mole fraction, divide by $1.6 \times 10^{22} \text{cm}^{-3}$.)

All the deformation and microhardness samples used to determine the

effects of varying amounts of radiation damage were cleaved from a high-purity single crystal grown at Oak Ridge by pulling from the melt. Six sets of samples were prepared for irradiation. A set consisted of one plate (6mm x 6mm x 2mm) which was used for the microhardness and absorption data, and five $\langle 100 \rangle$ parallelepipeds (1.5mm x 1.5mm x 8mm) which were used for compression flow stress data. Each set was wrapped in a single layer of aluminum foil in order to eliminate any possible bleaching effects of ambient light. The sets were irradiated in the Oklahoma State University Van de Graaff facility with 1.5 MeV electrons for various lengths of time. A beam current density of approximately 1.5×10^{13} electrons/cm² sec was used. The radiation dose for each set was determined from the F center absorption band, which was measured on the plate sample.

Table IV gives the engineering flow stress, the resolved flow stress measured under compression, and the average microhardness measured under a 15gm load for the irradiated samples.

Figure 14 compares the Vickers hardness to the resolved flow stress for both doped and irradiated samples. For the irradiated KCl, HV increases only 25% while τ_r goes up by a factor of 8 or 9. This is in contrast to our results for doped KCl. Johnston and Westbrook (reported by Johnston and Nadeau (9)) found a similar small increase in HV with a large increase in τ_r upon irradiation, for a number of alkali halides. These results suggest that the radiation damage products only blocked the primary slip system. Microhardness tests activate both the primary and secondary slip systems, and are less affected.

Figure 15 shows both the resolved and engineering flow stress versus the mole fraction F center concentration and interstitial

concentration, as measured by the F center optical absorption. The curve displays the $C^{\frac{1}{2}}$ dependence predicted by Fleischer's theory. Fleischer (10) has further shown theoretically that F centers and other symmetric defects should have little hardening effect. Interstitials and other defects which introduce tetragonal distortions into the lattice should markedly increase the flow stress. Nadeau (23) has verified that F centers cause little change in the flow stress by measurements made on additively colored crystals, which contain no interstitials. We have verified his results and extended them to crystals colored electrolytically by heating in an electric field. Such crystals, which contain F centers but no interstitials, show little change in flow stress over untreated specimens. Thus, hardening effects in irradiated crystals can be attributed to the presence of interstitials, and not of F centers.

TABLE IV
ENGINEERING FLOW STRESS, τ_e ; RESOLVED FLOW STRESS, τ_r ; VICKERS HARDNESS, HV; AND F CENTER CONCENTRATIONS, C, FOR IRRADIATED PURE KCl

C (ppm) ^a	τ_e (psi)	τ_r (kg/mm ²)	HV (kg/mm ²)
0	320	0.11	9.2
0	440	0.15	9.0
0	380	0.13	10.2
7.3	1240	0.43	11.4
17	1860	0.64	12.6
48	2460	0.85	13.2
60	2520	0.87	12.0
64	2700	0.93	13.2

^a Mole fraction

E. Discussion of Mechanical Results

Figure 16 shows the resolved flow stress versus $C^{\frac{1}{2}}$ for Sr doped KCl crystals and for irradiated KCl crystals where C is the mole fraction of the Sr impurity and the interstitial Cl respectively. Both sets of data show a linear dependence, but the slope is much steeper for irradiated crystals. From Equation 3 the slope should be G/n , where G is the shear modulus:

$$G = [\frac{1}{2}C_{44}(C_{11} - C_{12})]^{\frac{1}{2}} \quad (7)$$

In (7), the C's are the elastic constants as shown by Johnston et al. (24) for the $\{110\}\langle 110 \rangle$ primary slip system of the alkali halides. Equation 6 yields a value for G of $1.05 \times 10^3 \text{ kg/mm}^2$ for KCl. Using this value for G, the data of Figure 16 yield, for the irradiated and doped crystals respectively a value of $n = 12$ and 40. The value for the irradiated crystals is the same as that found by Sibley and Russell (6) for similar crystals, and is in good agreement with Fleischer's calculation for interstitial hardening. The larger value of n for the Sr doped crystals indicates that the Sr^{2+} -vacancy pair is less effective in hardening the crystal than the Cl^0 interstitial. For a divacancy, Fleischer predicted a value of 100 for n. While the Sr-vacancy pair is not directly comparable, it falls between the interstitial and the divacancy in hardening effectiveness. The hardening due to Sr doping most likely is due to the combined effects of the strain and electrostatic fields around the divalent Sr^{2+} -ion.

For both doped and irradiated KCl crystals, engineering flow stresses of 2500 to 2600 psi have been achieved with defect concentrations of 650 ppm divalent impurity and 65 ppm interstitial respectively.

Both techniques may be extended somewhat further or perhaps even combined. Sibley and Russell (6) have shown, however, that the increase in flow stress upon irradiation is smaller for Ca and Sr doped KCl than for pure KCl. The OSU-doped crystals will be investigated with respect to hardening under electron irradiation. Perhaps the most profitable approach for ir windows would be to use doped or irradiated polycrystalline material and take advantage of the Petch relation (Eq. 4), since either method will increase τ_0 . OSU Sr doped KCl will be made available for recrystallization experiments. We plan to investigate the flow stress on undoped recrystallized KCl from AFCRL.

IV. SUMMARY

The first crystal puller has been placed in operation and used to grow reagent grade undoped and Sr doped KCl crystals. A second puller and Bridgman system are nearly completed. The Bridgman system will allow us to compare crystals grown by both methods. We will grow crystals from different grades of starting material to determine if treatment processes are necessary; crystals for 10.6 μ m absorption measurements will be sent to AFCRL. We have found that the addition of 650 molar ppm Sr increases the engineering flow stress of reagent grade KCl from 300 psi to 2550 psi. Since these results are in good agreement with our earlier measurements on purified Oak Ridge material we conclude that the lower purity of reagent grade crystals is not a serious problem as far as mechanical properties are concerned. We have also irradiated high purity KCl from ORNL, and find that the engineering flow stress can be increased to 2700 psi for a radiation dose that produces 65 ppm Cl interstitials. Since both doping and irradiation should provide an additional

hardening mechanism in forged polycrystalline material, we are planning to irradiate forged material from AFCRL and to supply some Sr doped material to AFCRL for forging studies. Both doped and irradiated KCl single crystals have been sent to AFCRL for 10.6 μ m absorption measurements. We have measured the mechanical properties of both OH⁻ and O₂⁻ doped KCl crystals and find no significant degradation of the mechanical properties. We will further investigate optical and mechanical properties of O₂⁻ doped crystals, since there is some reason to believe that oxygen compounds may play a significant role in degrading performance at 10.6 μ m.

Publications and Thesis resulting from this work: J. A. Miller, J. R. Hopkins and J. J. Martin, "Flow Stress, Vickers Hardness and Wing Size for Pure and Doped KCl and for KCl:KBr Mixed Crystals", submitted to Physica Status Solidi (a); J. A. Miller, "Mechanical Properties of Potassium Chloride", unpublished M.S. thesis.

REFERENCES

1. F. Rosenberger, Mat. Res. Bull. 1, 55 (1966).
2. C. T. Butler et al., J. Chem. Phys. 45, 968 (1966).
3. C. T. Butler et al., "A Method for Purification and Growth of KCl Single Crystals", ORNL Report, ORNL-3906, Feb., 1966.
4. B. Fritz, F. Lüty and J. Anger, Z. Phys., 174 240 (1963).
5. H. Kelting and H. Witt, Z. Physik 126, 697 (1949).
6. W. A. Sibley and J. R. Russell, J. Appl. Phys. 36, 810 (1965).
7. J. J. Gilman and W. G. Johnston, Solid State Physics 13, 148 (1962).
8. W. A. Sibley and E. Sonder, J. Appl. Phys. 34, 2366 (1963).
9. W. G. Johnston and J. S. Nadeau, Aerospace Research Laboratories Report, ARL64-135, August, 1964.
10. R. L. Fleischer, Acta Met. 10, 835 (1962).
11. N. J. Petch, J. Iron and Steel Inst. 174, 25 (1953).
12. R. W. Rice, "High Energy Loser Windows", Semi-Annual Report No. 1, Naval Research Laboratory, December 31, 1972.
13. J. W. Davisson and W. H. Vaughan, Report of NRL Progress, p. 10, April, 1958.
14. G. W. Groves and M. E. Fine, J. Appl. Phys. 35, 3587 (1964).
15. R. W. Davidge, J. Mat. Sci. 2, 339 (1967).
16. M. Suszynska, Phys. Stat. Sol. A2, 635 (1970).
17. G. Y. Chin, L. G. Van Uitert, M. L. Green, and G. Zydzik, Scripta Met. 6, 475 (1972).
18. E. Aerts, S. Amelinckx, and W. Dekeyser, Acta Met. 7, 29 (1959).
19. W. A. Sibley et al., "Growth and Hardening of Alkali Halides for Use in Infrared Laser Windows", Semi-Annual Technical Report No. 1, Oklahoma State University, October 31, 1972.

20. J. Rolfe et al., Phys. Rev. 123, 447 (1961).
21. W. A. Sibley and E. Sonder, in Point Defects in Solids, (ed. J. H. Crawford and L. Slifkin) Plenum Press, 1972.
22. A. Smakula, Z. Fur Physik 59, 603 (1930).
23. J. S. Nadeau, J. Appl. Phys. 34, 2248 (1963).
24. W. G. Johnston, J. S. Nadeau, and R. L. Fleischer, J. Phys. Soc. Japan (Suppl. I) 18, 7 (1963).

FIGURE CAPTIONS

- Fig. 1. Schematic Diagram of the Model 1 Puller.
- Fig. 2. Schematic Diagram of the Model 2 Puller.
- Fig. 3. Three Sr Doped Reagent Grade Crystals Grown in the Model 1 Puller. The scale is in cm.
- Fig. 4. Crystal Sr Content Versus Melt Sr Content.
- Fig. 5. Stress-Strain Curve for a Typical Purified KCl Crystal as Measured Under Compression.
- Fig. 6. Diagram for a Four Point Bending Jig.
- Fig. 7. Stress-Strain Curve for a Pure KCl Crystal as Measured Under Four Point Bending.
- Fig. 8. Comparison of the Flow Stress from a Four Point Bend Test to the Flow Stress from a Uniaxial Compression Test.
- Fig. 9. A Dislocation Rosette of a 50gm Load Indentation on KCl:Sr.
- Fig. 10. The Vickers Microhardness, HV, Versus the Resolved Flow Stress, τ_r , Is Shown for Pure KBr, Pure KCl, KCl:Ca, KCl:Sr and $\text{KCl}_x\text{Br}_{1-x}$ Crystals.
- Fig. 11. The Dislocation Rosette Wing Size Versus Indentor Load.
- Fig. 12. A Plot of Resolved Flow Stress Versus $100/W_0$.
- Fig. 13. The Resolved Flow Stress, τ_r , Versus the Mole Fraction Sr Concentration, C. The Engineering Flow Stress Is on the Right.
- Fig. 14. Vickers Hardness Versus Resolved Flow Stress for Irradiated Pure KCl Crystals (lower curve) and for Doped KCl Crystals (upper curve).

Fig. 15. The Resolved Flow Stress, τ_r , Versus Radiation Damage as Measured by the Mole Fraction F Center Concentration, C. The Engineering Flow Stress Is on the Right.

Fig. 16. The Resolved Flow Stress, τ_r , Versus the Square Root of Either the Sr Concentration or Radiation Damage, C.

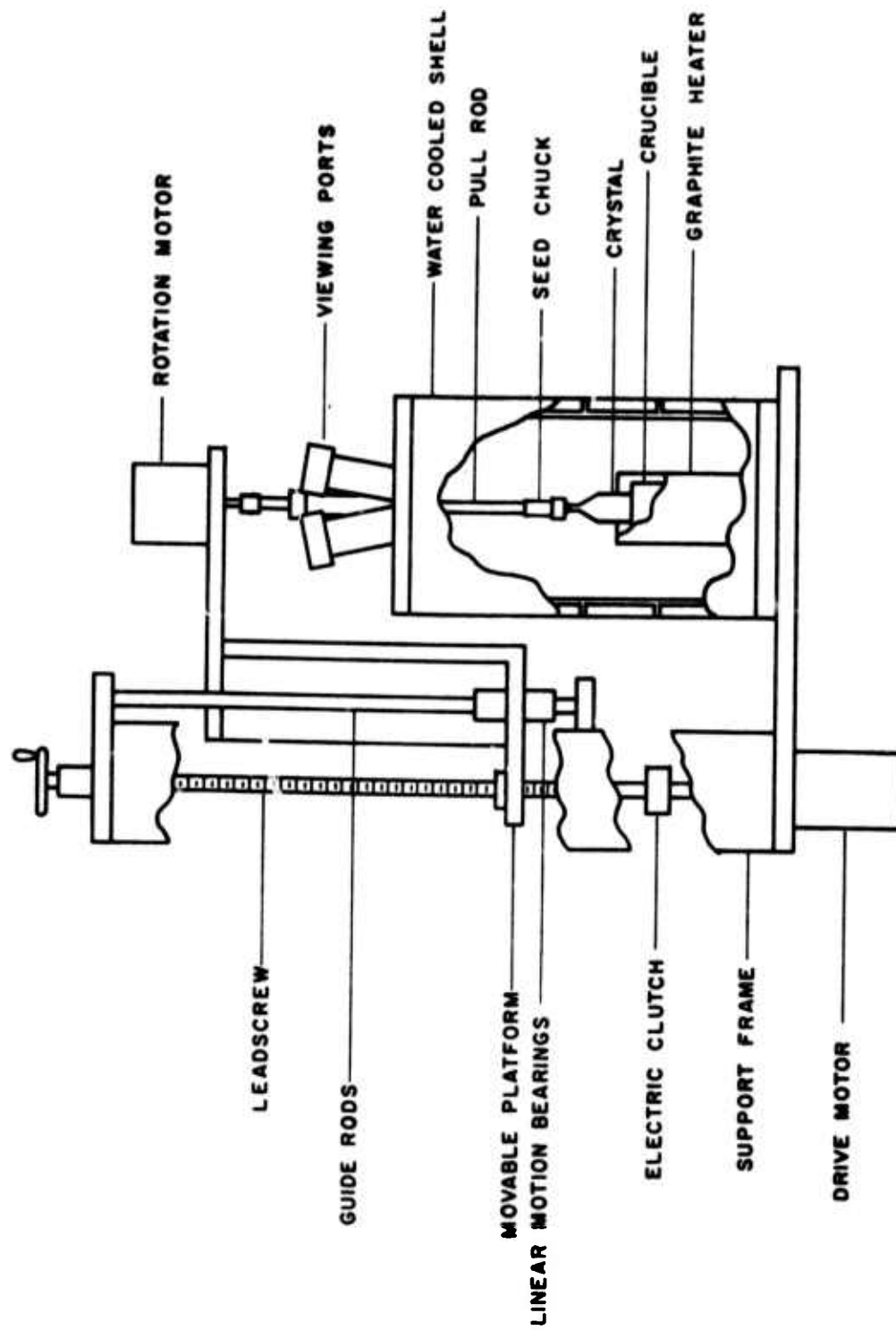
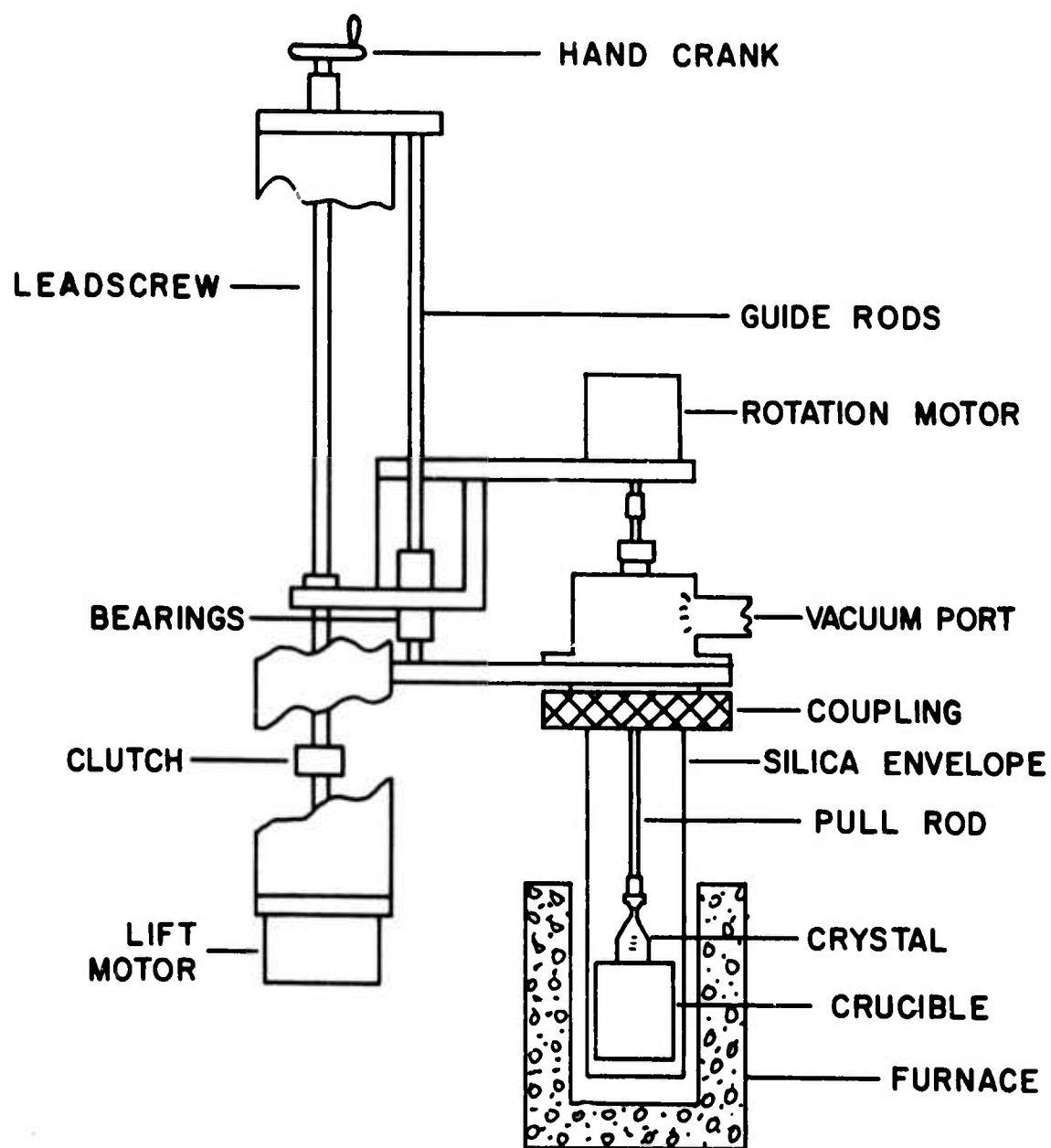


Figure 1. Schematic Diagram of the Model 1 Puller



MARK II CRYSTAL PULLER

Figure 2. Schematic Diagram of the Model 2 Puller

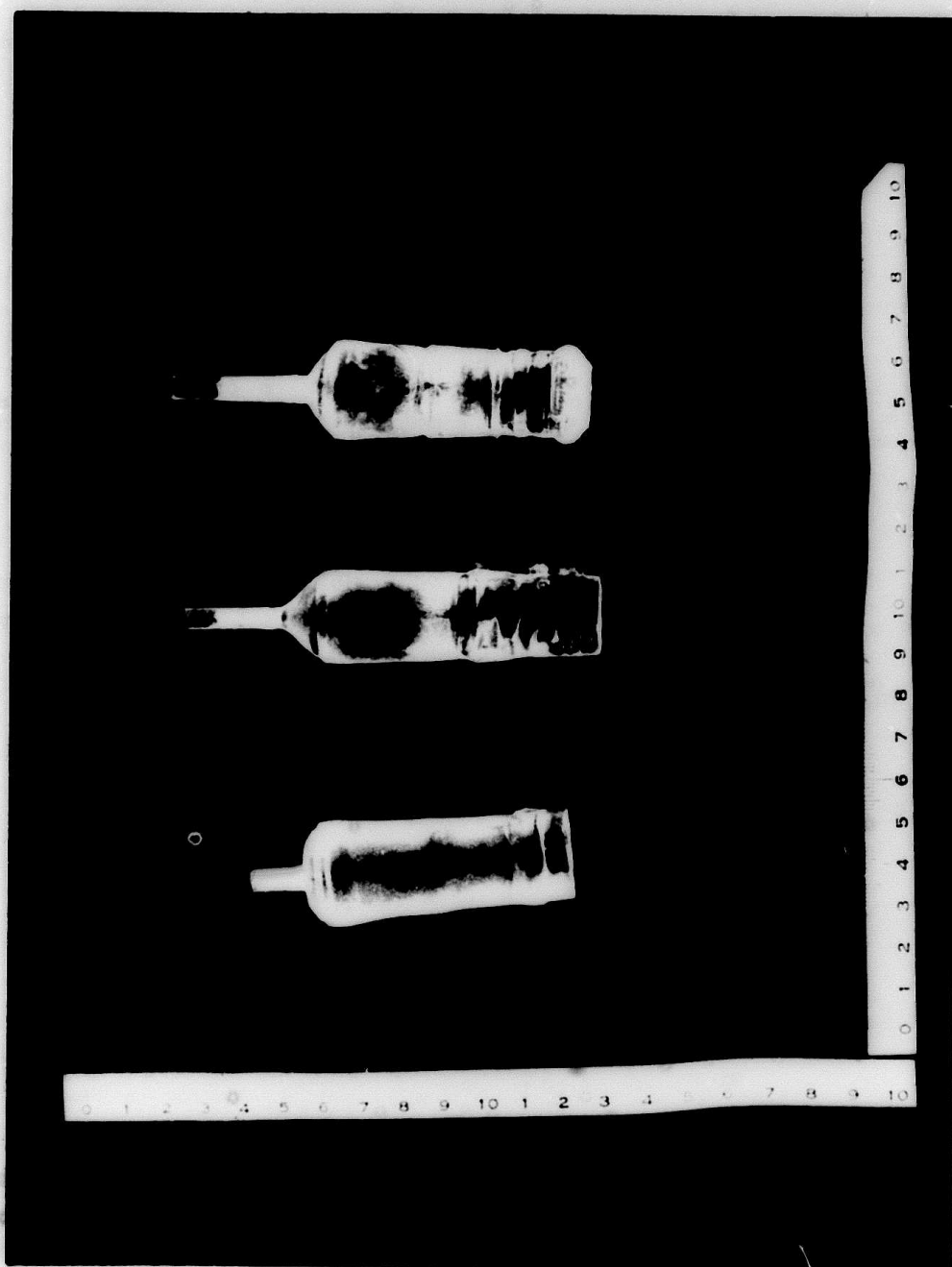


Figure 3. Three Sr Doped Reagent Grade Crystals Grown in the Model 1 Puller. The scale is in cm

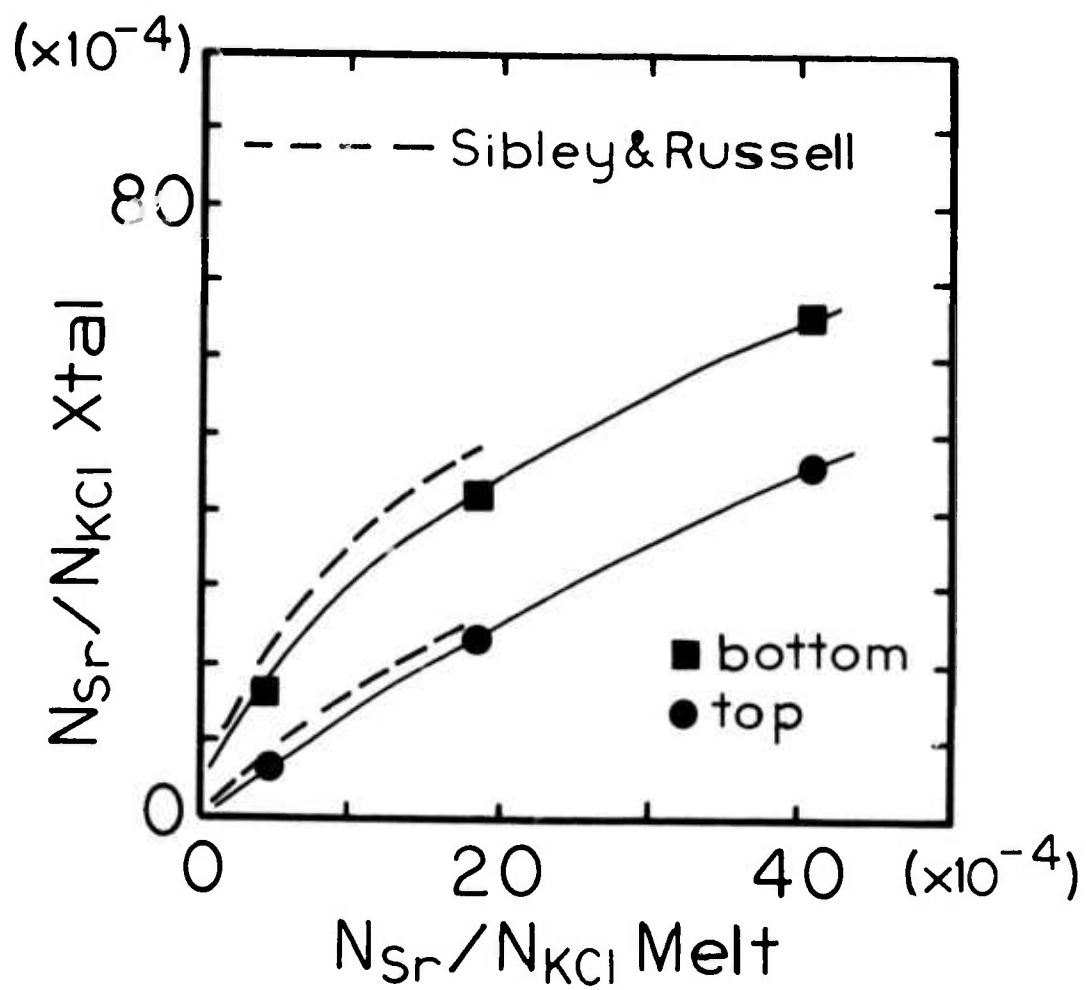


Figure 4. Crystal Sr Content Versus Melt Sr Content

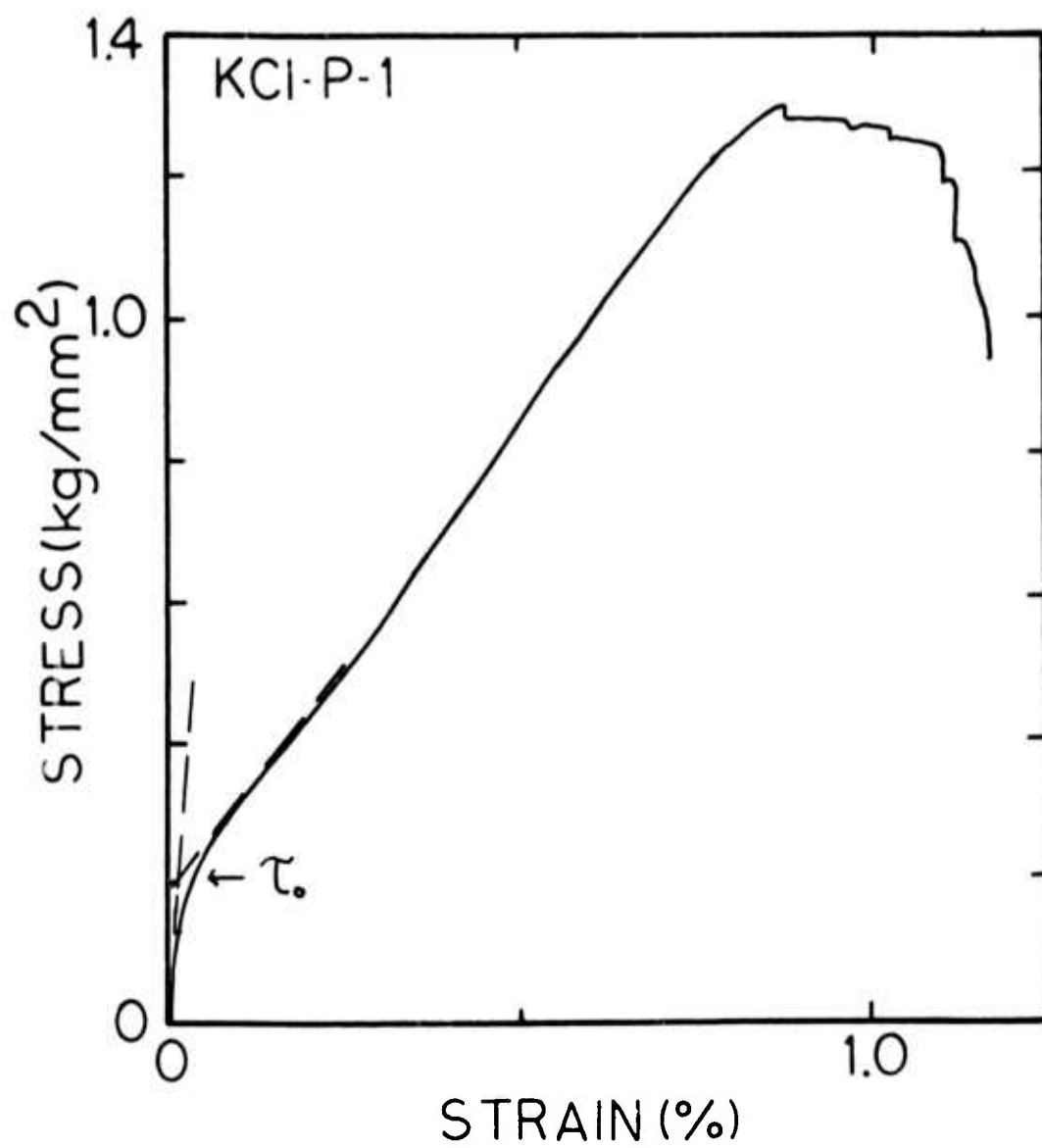


Figure 5. Stress-Strain Curve for a Typical Purified KCl Crystal as Measured Under Compression

Total Force = P

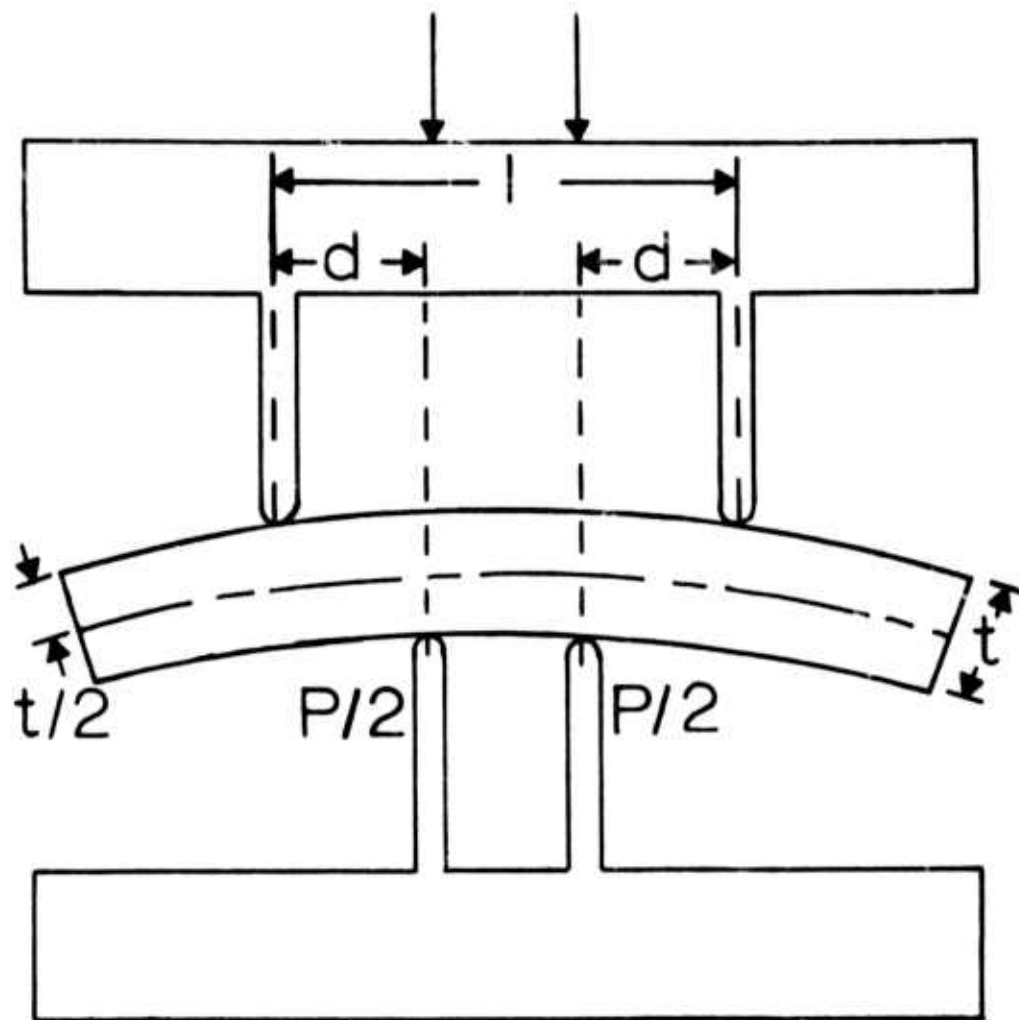


Figure 6. Diagram for a Four Point Bending Jig

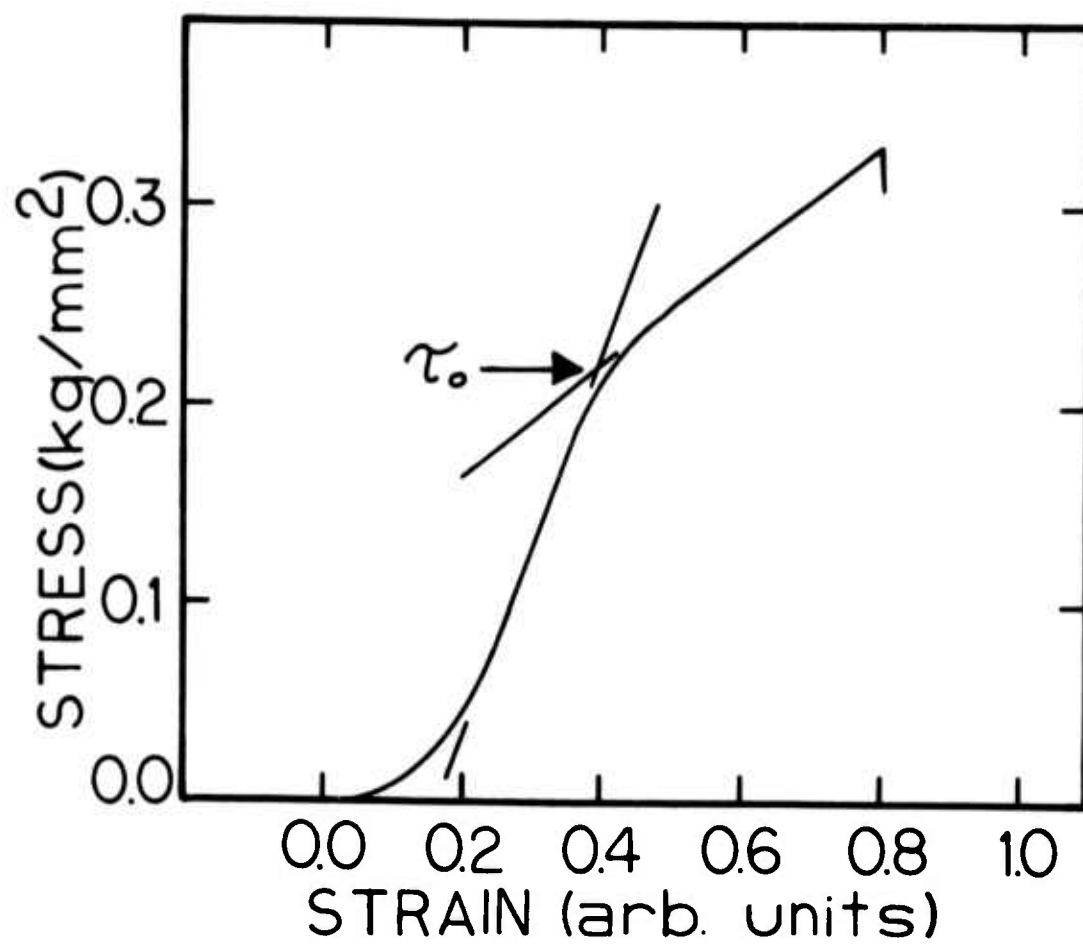


Figure 7. Stress-Strain Curve for a Pure KCl Crystal as Measured Under 4-Point Bending

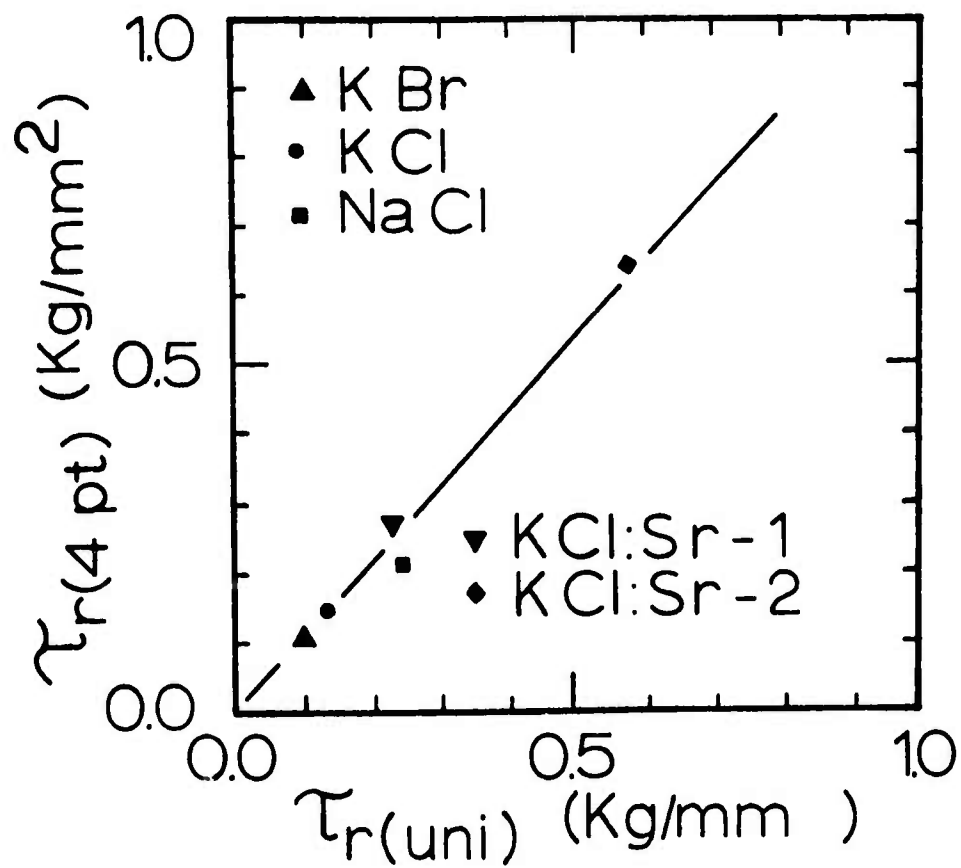


Figure 8. Comparison of the Flow Stress From a Four Point Bend Test to the Flow Stress From a Uniaxial Compression Test

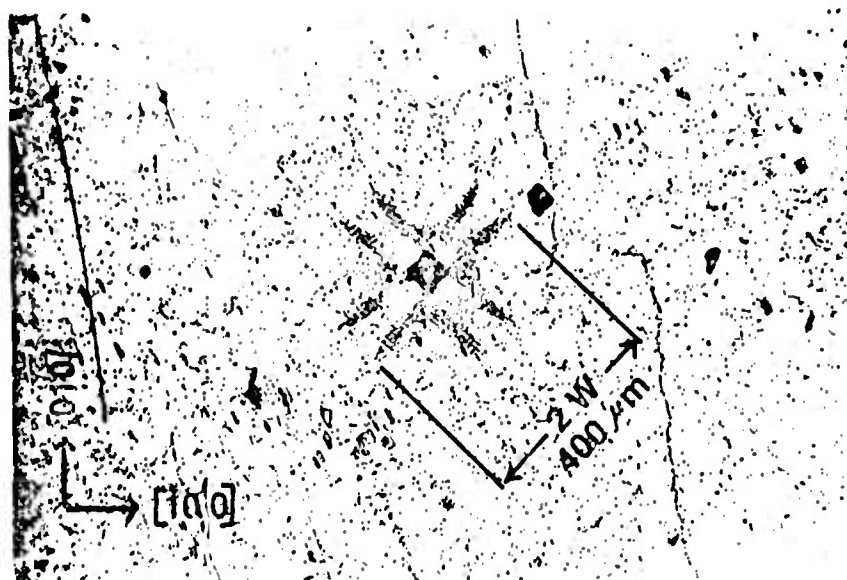


Figure 9. A Dislocation Rosette of a 50gm Load Indentation on KCl:Sr

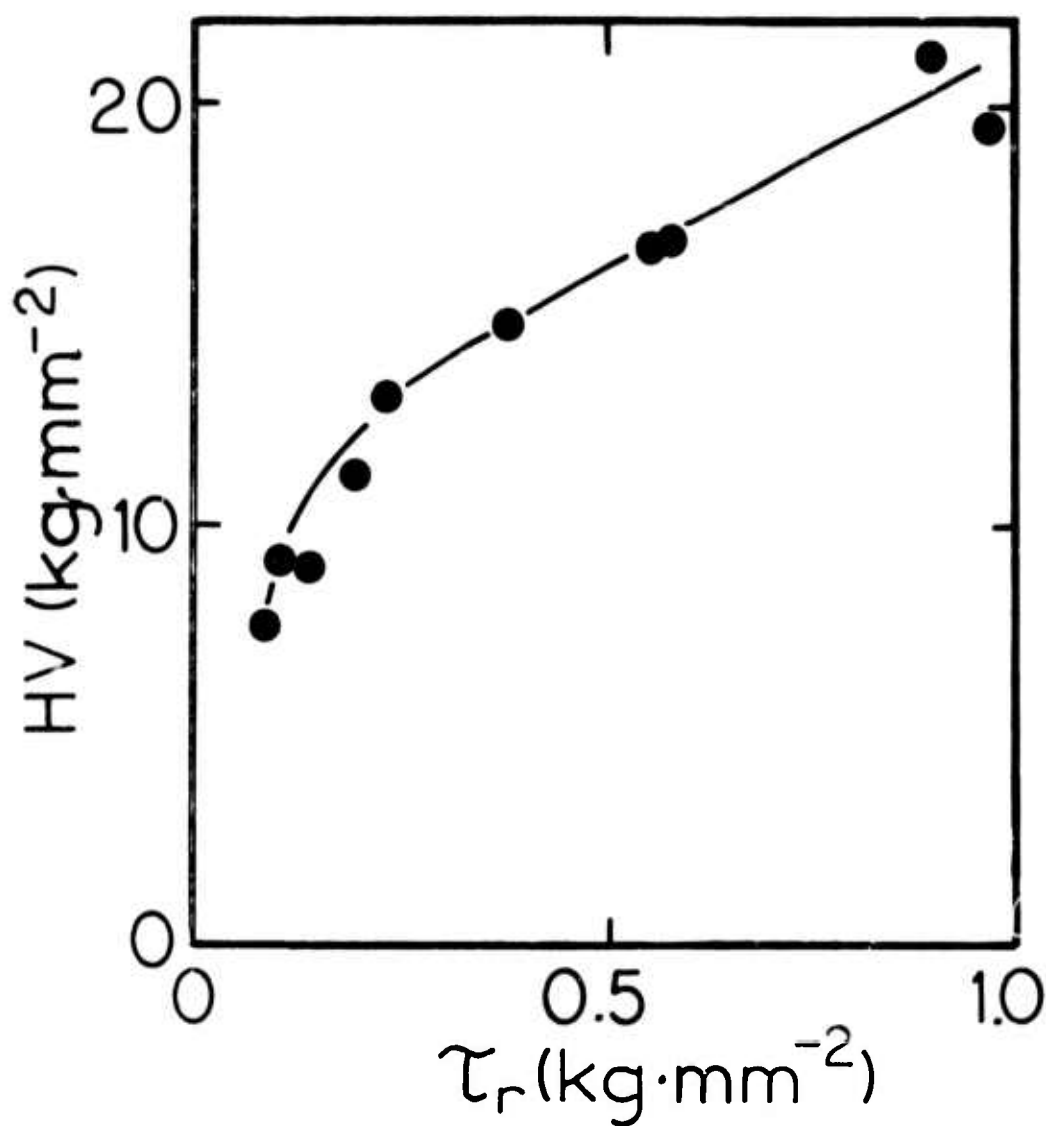


Figure 10. The Vickers Microhardness, HV, Versus the Resolved Flow Stress, τ_r , is Shown for Pure KBr, Pure KCl, KCl:Ca, KCl:Sr and $\text{KCl}_x\text{Br}_{1-x}$ Crystals

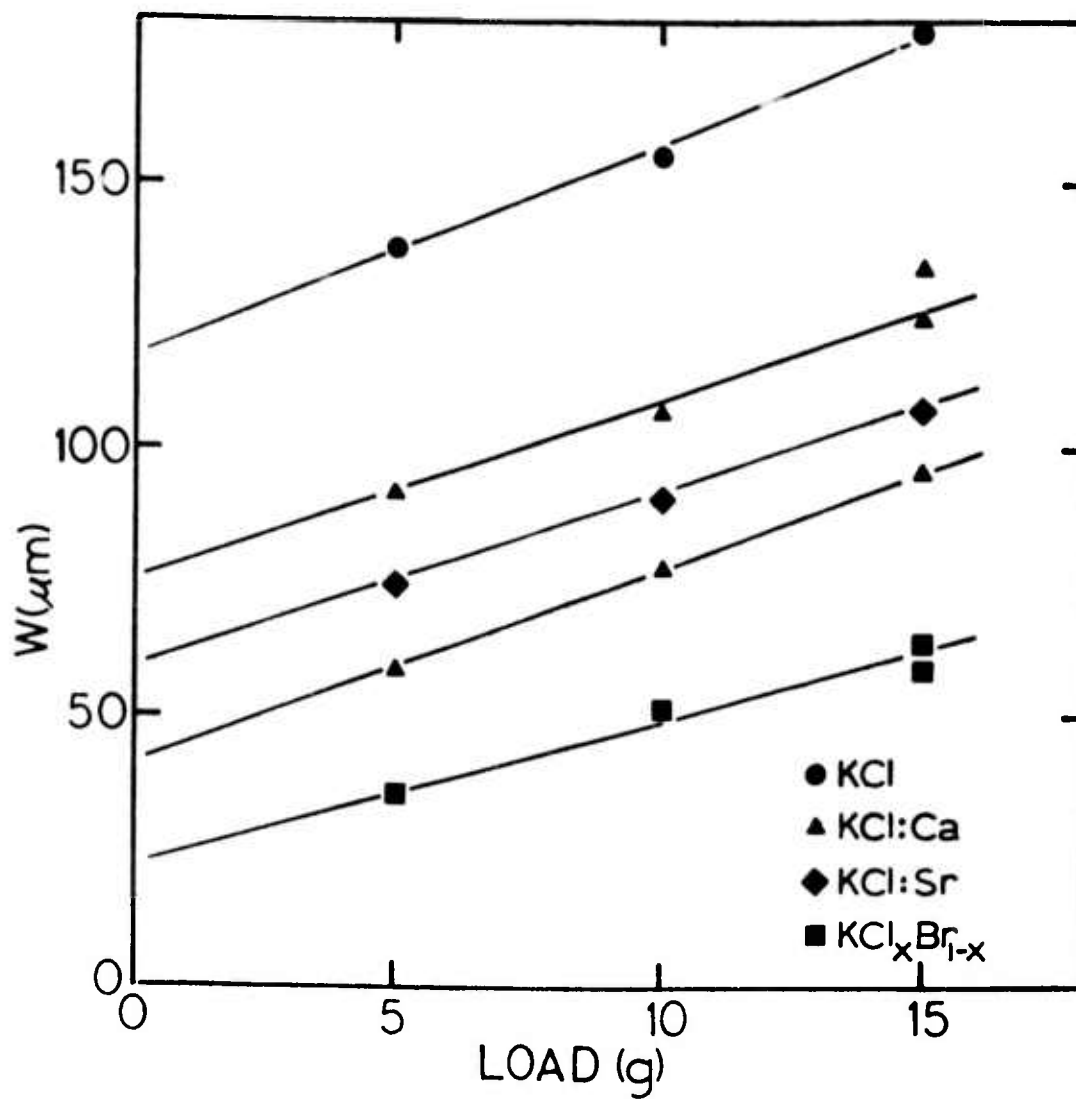


Figure 11. The Dislocation Rosette Wing Size Versus Indentor Load

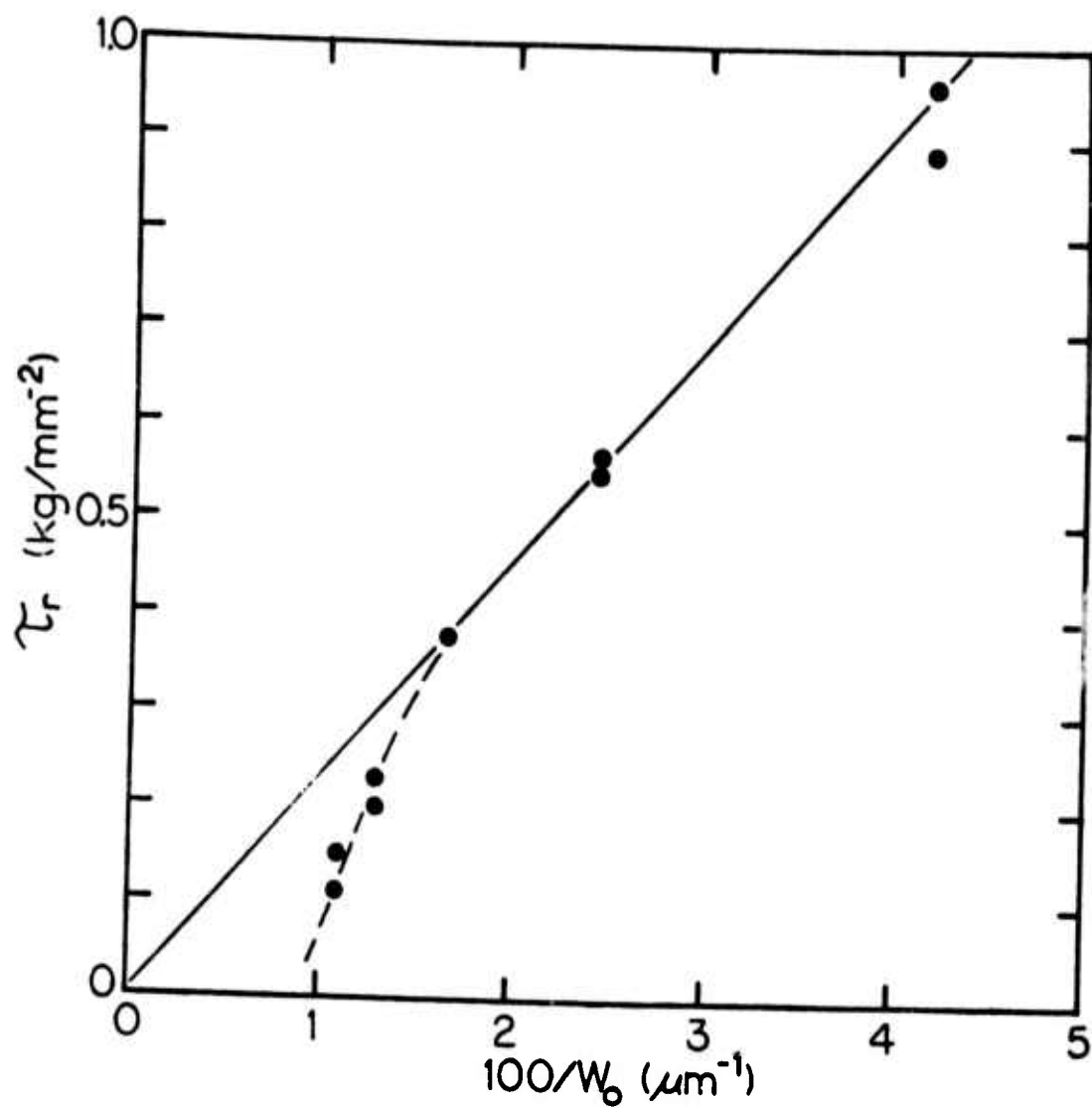


Figure 12. A Plot of Resolved Flow Stress Versus $100/w_0$.

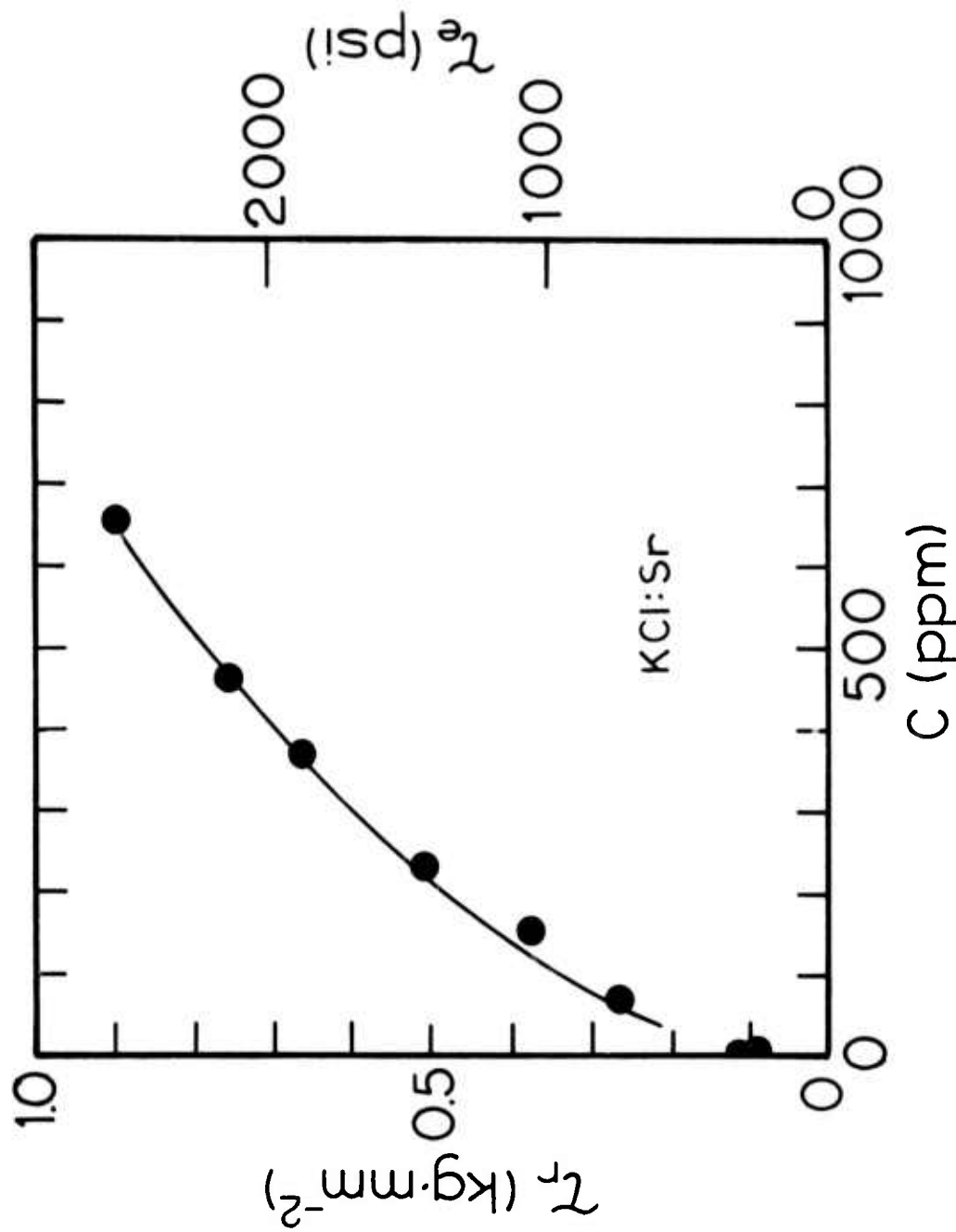


Figure 13. The Resolved Flow Stress, τ_r , Versus the Mole Fraction Sr Concentration, C .
The Engineering Flow Stress is on the Right

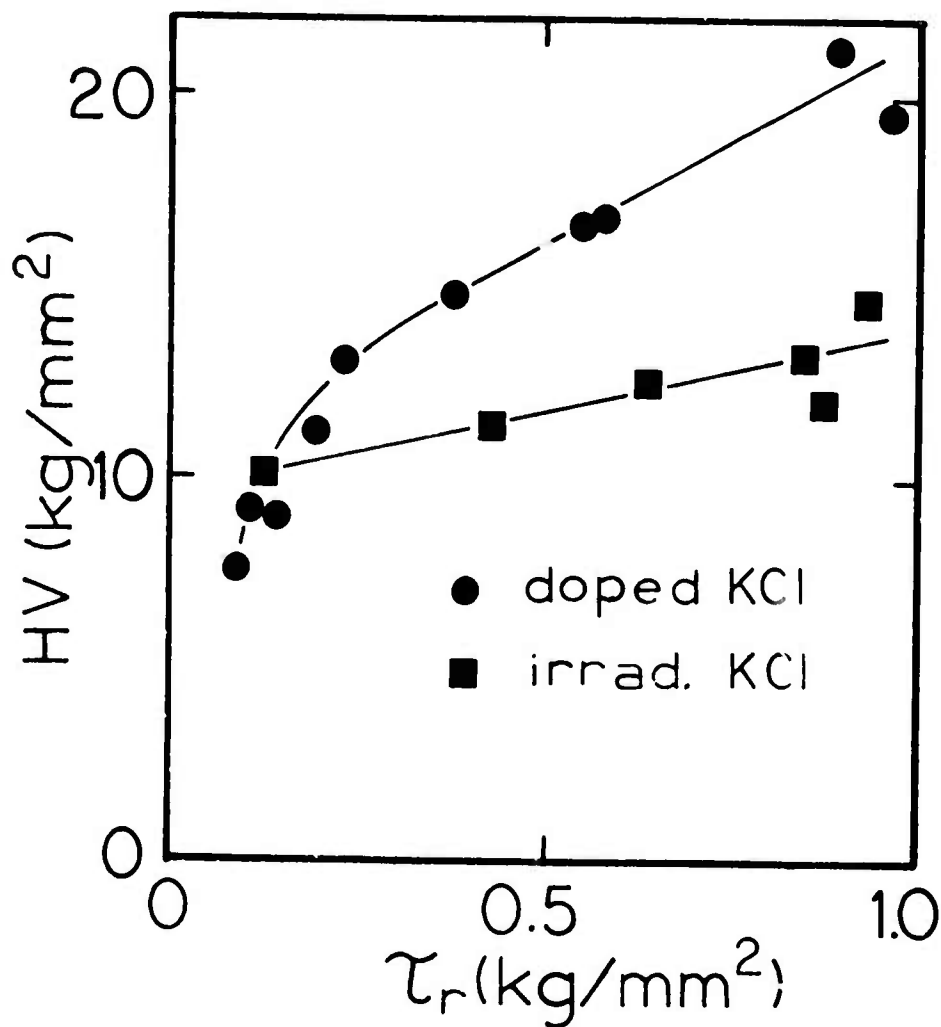


Figure 14. Vickers Hardness Versus Resolved Flow Stress for Irradiated Pure KCl Crystals (lower curve) and for Doped KCl Crystals (upper curve)

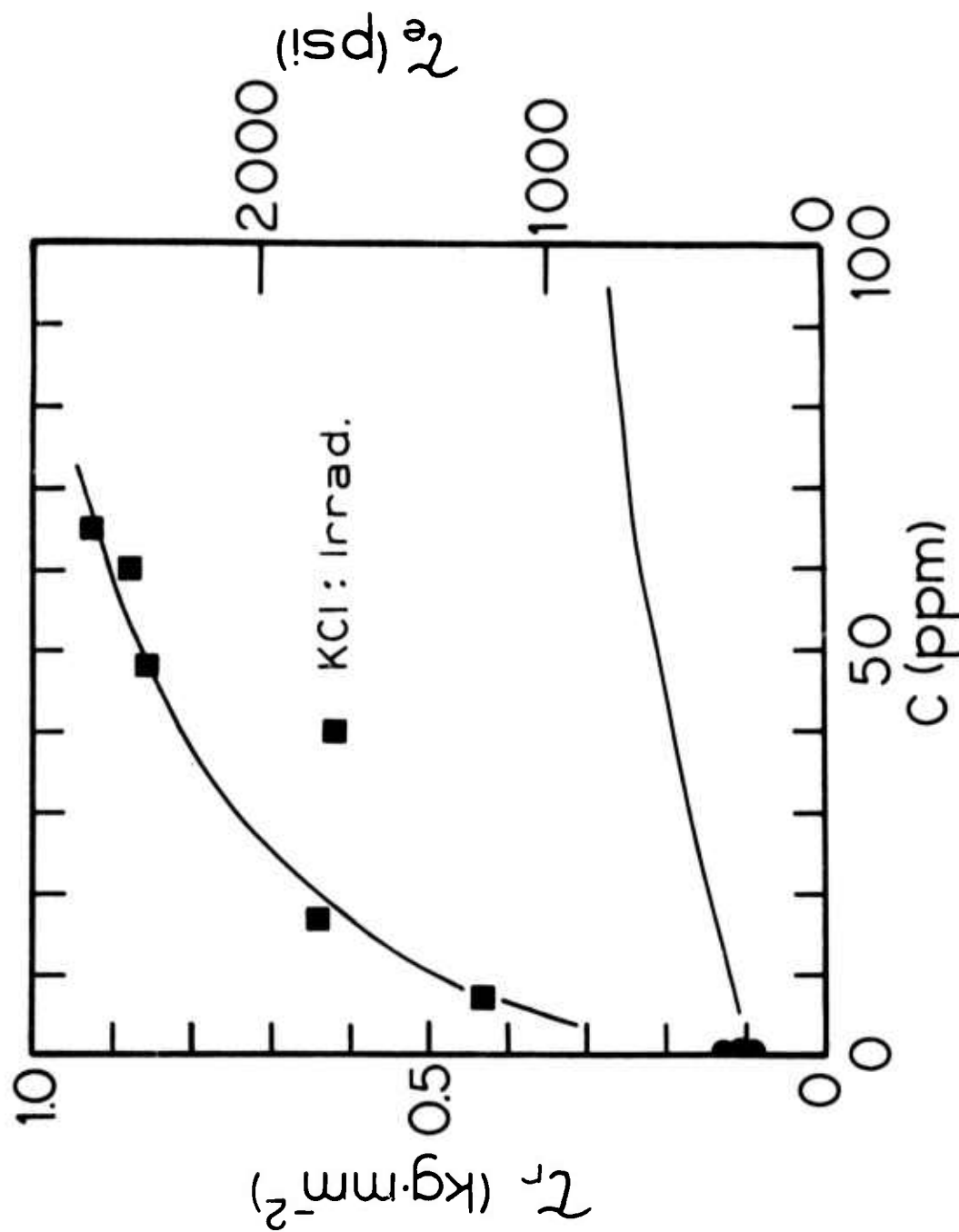


Figure 15. The Resolved Flow Stress, τ_r , Versus Radiation Damage as Measured by the Mole Fraction F Center Concentration, C. The Engineering Stress is on the Right

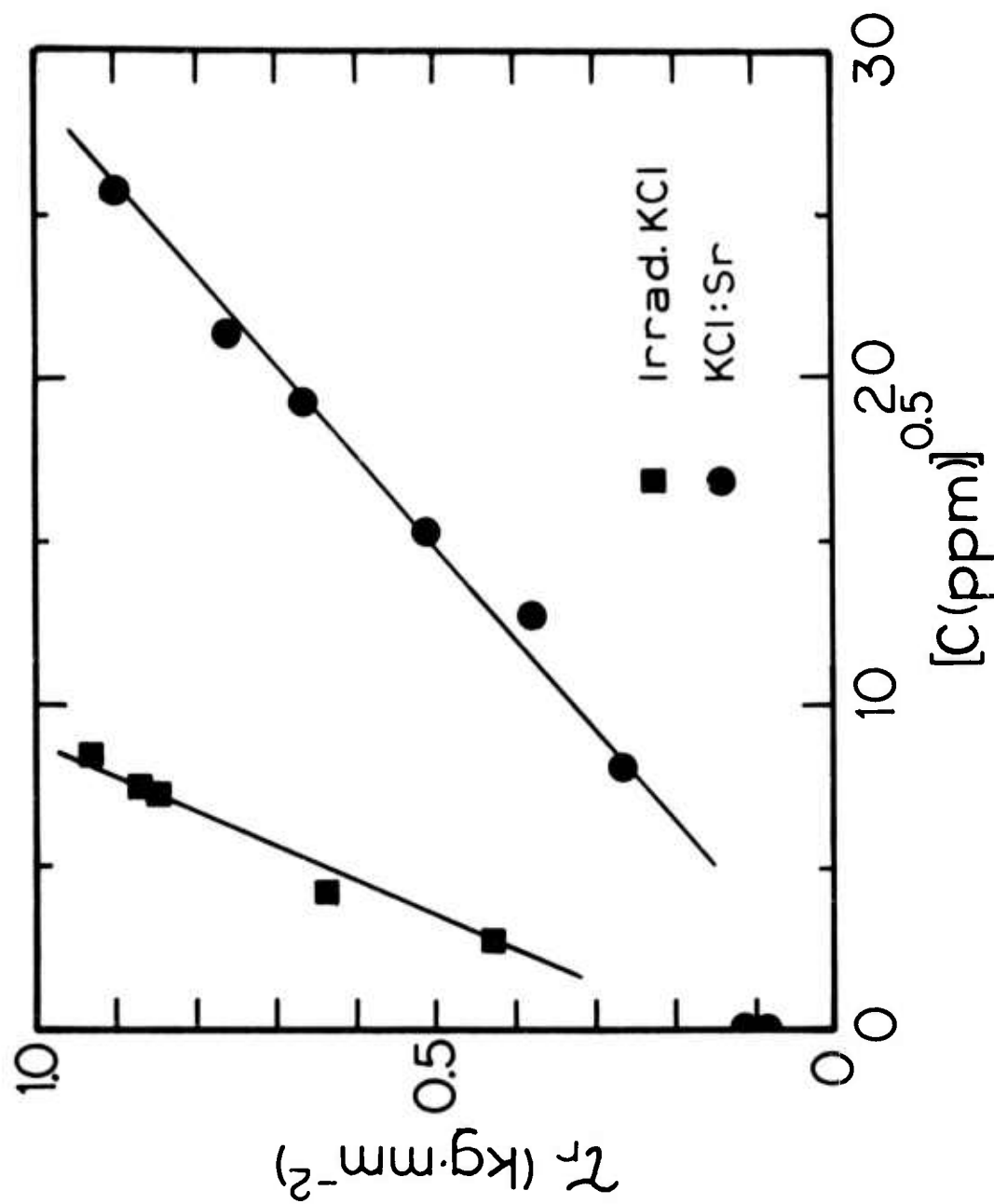


Figure 16. The Resolved Flow Stress, τ_r , Versus the Square Root of Either the Sr Concentration or Radiation Damage, C